J. Korean Soc. Tribol. Lubr. Eng., Vol. 31, No. 2, April 2015, pp. 50~55 ISSN 1229-4845(Print) · 2287-4666(Online)
Journal of the Korean Society of Tribologists & Lubrication Engineers http://Journal.kstle.or.kr

DOI http://dx.doi.org/10.9725/kstle.2015.31.2.50

Tribology Characteristics in 200 μm of Hexagonal Array Dimple Pattern

W. S. Choi[1†], Angga S. H.[1], S. H. Kwon[1], S. G. Kwon[1], J. M. Park[1], J. S. Kim[1], S. W. Chung[1] and Y. H. Chae[2]

[1]*Dept. of Bio Industrial Machinery Engineering, Pusan National University, Korea*
[2]*School. of Mechanical Engineering, Kyungpook National University, Korea*

(Received November 5, 2014; Revised March 31, 2015; Accepted April 1, 2015)

Abstract – This study investigates the effects of a pattern of 200 μm dimples in a hexagonal array on tribological characteristics. A textured surface might reduce the friction coefficient and wear caused by third-body abrasion and thus improve the tribological performance. There are three friction conditions based on the Stribeck curve: boundary friction, mixed friction, and fluid friction conditions. In this experiment, we investigate the friction characteristics by carrying out the friction tests at sliding speeds ranging from 0.06 to 0.34 m/s and normal load ranging from 10 to 100 N. We create dimple surfaces for texturing by using the photolithography method. There are three kinds of specimens with different dimple densities ranging from 10% to 30%. The dimple density on the surface area is the one of the important factors affecting friction characteristics. Friction coefficient generally decreases with an increase in the velocity and load, indicating that the lubrication regime changes depending on the load and velocity. The fluid friction regime is fully developed, as indicated by the duty number graph. Fluid friction occurs at a velocity of 0.14-0.26 m/s. The best performance is seen at 10% dimple density and 200 μm dimple circle in the hexagonal array.

Keywords – friction coefficient, surface texturing, dimple pattern, stribeck

1. Introduction

Approximately 40% of the total energy loss results from engine friction and wear loss; hence, friction and wear must be reduced to improve fuel consumption. Surface texturing is an emerging method for effectively improving the tribological performance of mechanical components.

Surface texturing is one of the methods to reduce friction in tribology [1]. This method is also used to improve function and performance by marking in the surface by chemical or mechanical varied method. It has been studied that engineered surface was showed since 1940's.

Recently, research was carried out on contact areas within a pattern by developing a semi-contact material process. Nanopattern formation on silicon wafers reduces the friction during sliding contact motion. Formation of microdimple patterns using a razor is a technique known to decrease the friction coefficient and seizure on the SiC ceramic materials.

Surface texturing onto a solid material during sliding contact can modify the friction characteristics of the material. Surface texturing to create square-patterned dimples or pores has been reported to reduce the coefficient of friction due to lubricant retention. Surface texturing is also useful for reducing the wear of materials, because worn fragments fall into the pores or holes during sliding, thereby lowering third-body abrasion action. It is also known to cause resistance due to the hydrodynamic disturbance of the lubricant during sliding motions, resulting in an increased coefficient of friction [2]. Therefore, it can be assumed that the sur-

†Corresponding author : choi@pusan.ac.kr
Tel: +82-55-350-5651, Fax: +82-55-350-5429

face texturing density and depth of the hole have roles to play in surface texturing for low-friction materials.

The condition underlying surface texturing were divided by worn fragments trapping, lubricant reservoir and hydrodynamic, but it also depends on the size and density of the texture, as well as the depth of the pattern even if each theory about friction characteristic on surface texturing are reasonable [3]. Therefore, there are not appearing comprehends for surface texturing. The present study tested the friction coefficient for 200 μm surface dimple patterns. In several studies, grooves were created by a mechanical process or by using a laser. A different method is applied in this study, where photolithography is used to produce the dimple. The mechanism of surface texturing is decided by a worn fragments trapping, lubricant reservoir and hydrodynamic, but each theory has propriety, they are depend on the density, depth, dimension of the pattern. Thus, there has been no complete study on surface texturing till date [4-9].

Scaraggi *et al.* reported that different surfaces with different micro hole depths exist, minimizing friction at the interface [10]. Wakuda *et al*. also reported that distribution of micro-dimples is an important factor against frictional characteristic [11].

Stribeck investigated friction as a function of load and speed, and published his research in the early 1900s [12]. It possible to identify a point of minimum friction and apply it to a lubrication system. He also showed that the friction for sliding bearings was high at low speeds, decreased to a minimum when metal-to-metal contact was ceased, and then increased again at higher speeds. Stribeck systematically studied the variation in friction between two liquid-lubricated surfaces as a function of speed for different loads. The graphs of friction force reported by Stribeck stem from a carefully conducted, wide-ranging series of experiments on journal bearings. They clearly show the minimum value of friction, now known as the transition between full fluid-film lubrication and some solid asperity interactions. The original results published by Stribeck best fit the classical "Stribeck curve". The friction regimes for sliding of lubricated surfaces are traditionally categorized into solid/boundary friction, mixed friction, and fluid friction, on the basis of the "Stribeck curve" [13].

Table 1. Test conditions

Parameters	Conditions
Contact type	Pin-on-Disk
Disk material	Bearing steel
Pin material	Bearing steel
Size of dimple for pin [μm]	200
Density of dimple for pin [%]	10-30
Depth of dimple for pin [μm]	2
Surface roughness – Pin before fabrication[μm]	0.008Ra, 0.016Ra
Surface roughness – Disk [μm]	0.039Ra, 0.052Ra
Diameter of pin [mm]	4
Diameter of sliding track [mm]	40
Normal load range [N]	20-100
Pressure range [MPa]	0.25-2.05
Speed range [m/s]	0.06-0.34
Lubricant	Paraffin oil
Temperature	Room temperature

The dimple circle of 200 μm was chosen for the preliminary study, which assumed has efficiently distribute on the 4 mm pin surface than the others. This assumption is according to the trial and error on the prototype specimens made. The dimples resemble the bulges and are distributed evenly on the surface of the pin. In this study, the friction coefficient in a hexagonal array of 200 μm micro-dimple patterns will be investigated and discussed.

2. Materials and Methods

The pin specimen was steel, with 4 mm diameter and 1 mm thickness. Micro-dimple patterns were formed on its surface by photolithography, via wet etching. The dimple circle of the prepared film photo mask was designed to be 200 μm. The test piece was made by using NaCl electrolyte and the dimple depth

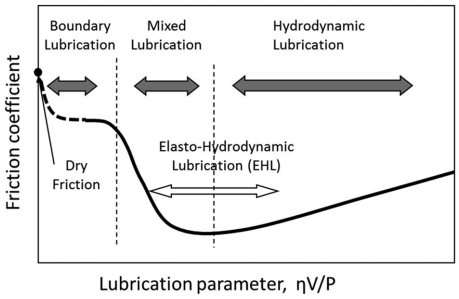

Fig. 1. Stribeck's curve.

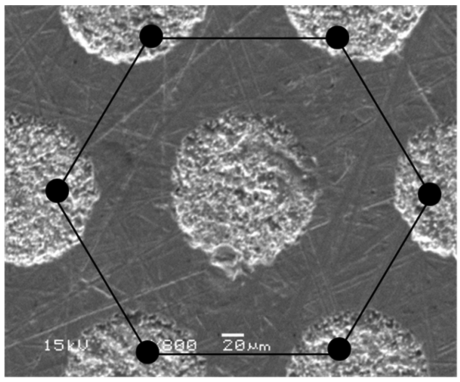

Fig. 3. Hexagonal array observed under an electron microscope.

was about 2 μm within the hexagonal array pattern. The disk material was bearing steel, with 60 mm diameter and 5 mm thickness; the surface roughness was 0.039 mmRa after polishing.

Fig. 1 shows the Stribeck curve [14]. Each friction region is clearly described by lubrication parameters. In this study, the duty number was used as the lubrication parameter. Duty number is a dimensionless number as a function of velocity in m/s, viscosity in Pa s, load in N, and pin diameter in μm. The duty number is expressed as follows:

$$duty\ \ number = \frac{viscosity \times velocity \times diameter}{load}$$

Fig. 2 shows the frictional test set and the data recording. A computer was used for data recording. The sensor (load cell) measured the surface friction in 60 s at 0.1 s time intervals for each variation. Seven variations of load were given to the test specimen, and the velocity, too, was varied for each loading. The test conditions are shown in Table 1, with the density ranging from 10% to 30% and the velocity ranging from 0.06 m/s to 0.34 m/s

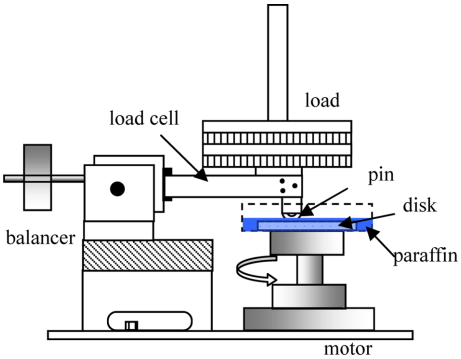

Fig. 2. Schematic of experimental apparatus.

Both the surfaces were brought in contact in the perpendicular position. Position adjustment was made using the water level. Maintaining the pin at the level position is very important because the load must be maintained at the normal position, which is the position perpendicular to the contact surface.

The perpendicular position will help in maintaining the normal force distribution on the contact surface. Besides, the stability of the pin affects the load cell readability. For lubricating the pin, about 20 ml of paraffin oil is used. The lubricant must be flooded and cover the contact surface between the pin and the disk. Fig. 3 shows the dimple pattern in the hexagonal array, as observed under an electron microscope with 800x magnification. The dimples are arranged in the symmetrically hexagon, and form a honeycomb-like structure when connected by an imaginary line. This configuration provides symmetry in the dimple distribution.

The dimple density is the ratio of dimple area to the total pin area, and hence, the dimple density is proportional to the number of dimples.

3. Results and Discussion

3-1. Friction characteristics

The experiment results revealed several graphical tendencies in each variation. In the initial stage of the

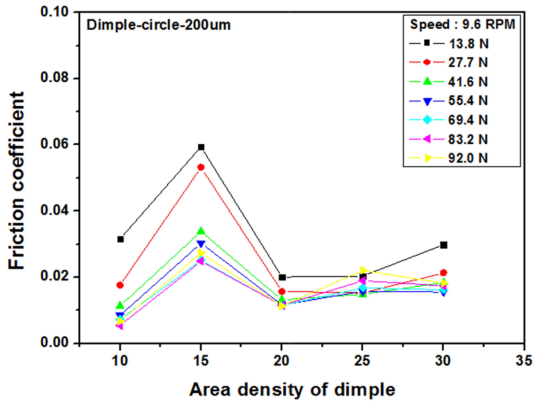

Fig. 4. Friction coefficient as a function of density at 9.6 rpm.

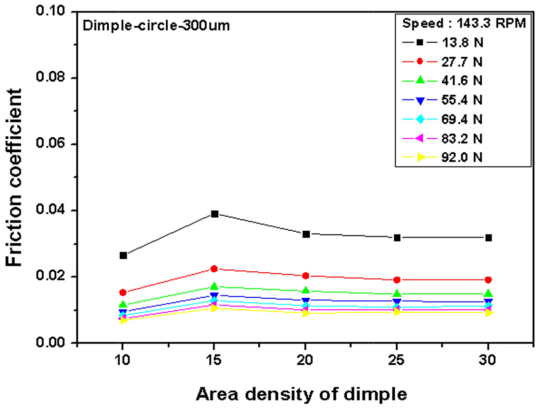

Fig. 6. Friction coefficient as a function of density at 143.3 rpm.

experiment, the sliding speed was 9.6 rpm. Fig. 4 depicts the friction coefficient as a function of density at 9.6 rpm. A dimple density of 10% provided the lowest friction coefficient at a load ranging from 41.6 N to 92 N; at lower loads ranging from 13.8 N to 27.7 N, a high friction coefficient was observed. Fluctuations in the friction coefficient were seen at 25% and 30% dimple density, when load increments were provided.

At higher rpm, the friction coefficient was stable as seen in Fig. 5 and Fig. 6. No significant fluctuation in the friction coefficient occurred under these conditions. At 15% dimple density, variations in the sliding speed significantly affected the friction coefficient.

For 20% dimple density, friction coefficient fluctuations occurred at 143.3 rpm and 27.7 N of load. Comparing Fig. 5 to Fig. 6, the friction coefficient significantly increased when the sliding speed increased from 86 rpm to 143.3 rpm (0.22-0.36 m/s); further, dimple densities other than 20% caused a decrease in the friction coefficient when the velocity was. This phenomenon indicated that velocity is critical for the pin with 20% dimple density, under 27.7 N of load.

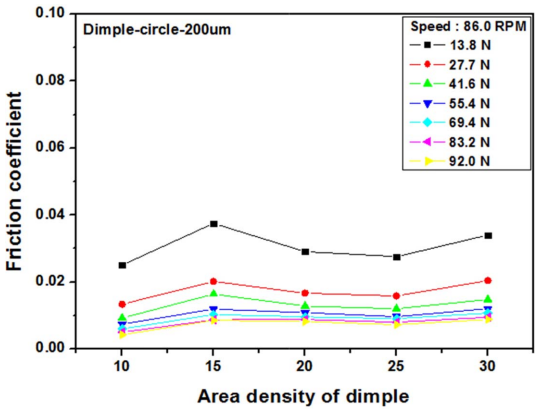

Fig. 5. Friction coefficient as a function of density at 86.0 rpm.

Velocity and load increment had important roles to play in this test, as they both affected the friction coefficient [12-13]. The graph indicated that the friction coefficient differed with the area density of the dimples. Among the five pin specimens considered, the pin with 10% density showed the best performance. The lowest friction coefficient was observed when the sliding speed was in the range 9.6 rpm to 143.3 rpm.

The friction initially decreased, reaching a minimum, and then increased with an increment in the velocity and load [12].

There are three kinds of friction as classified on the basis of the Stribeck curve: boundary friction, mixed friction, and fluid friction [13]. Boundary friction occurs when two surfaces in contact rub against each other. Under this condition, third-body contact may occur.

The dimpled pin surface plays the main role in the friction, under the boundary friction conditions. The third-body contact is potentially reduced [3] in this case, as shown in Fig. 7, on the graph for 15% dimple density. Under a load of 13.8 N and sliding speed of

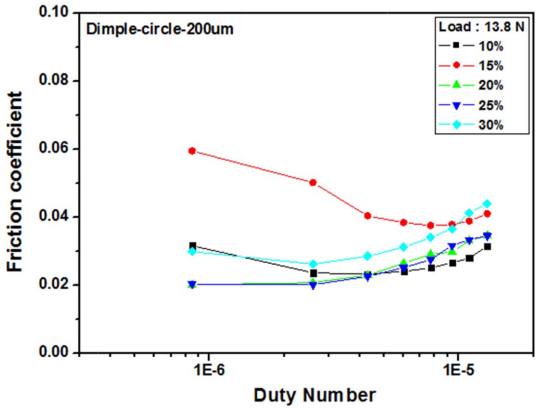

Fig. 7. Friction coefficient as a function of duty number at 13.8 N.

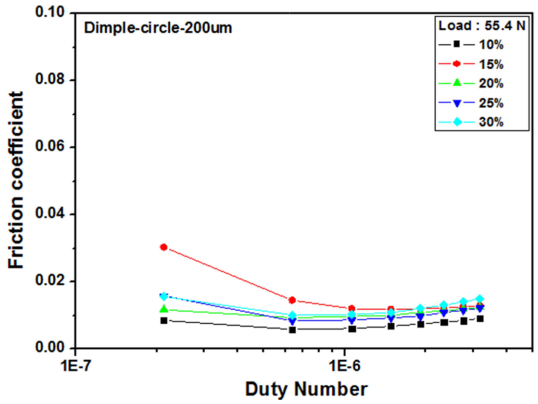

Fig. 8. Friction coefficient as a function of duty number at 55.4N.

9.6-143.3 rpm, three regions of friction can be seen. The friction coefficient at the lowest sliding speed is initially high, and then decreases to a minimum with increasing sliding speed. The minimum friction coefficient is observed when the sliding speed s varied between 86 rpm and 105.1 rpm (0.22-0.26 m/s).

Fig. 7 shows that another pin with a different dimple density shows similar graph tendency for the lowest load. Fig. 8 and Fig. 9 show changes in the graph tendencies.

The dimpled pin with 10% density showed the best performance at a higher load and sliding speed. The friction coefficient was the lowest when the load increased, as shown in Fig. 8 and 9. The duty number remained almost constant with an increase in velocity.

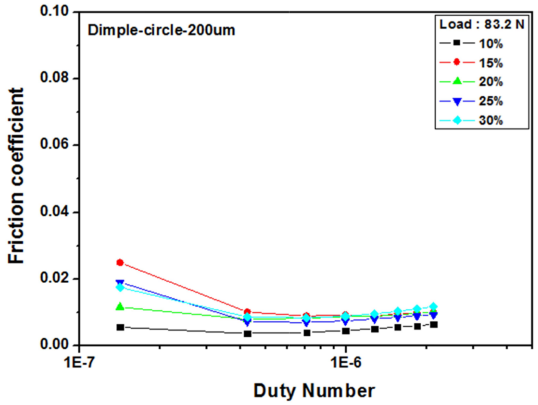

Fig. 9. Friction coefficient as a function of duty number at 83.2 N.

With increasing load and sliding speed, the friction coefficient slope for 10% dimple density was a near-straight line along the horizontal axis. Under 83.2 N load, the friction coefficient was significantly different from that for the other pins, as shown in Fig. 9. Even at a lower sliding speed and load, several pins showed a friction coefficient smaller than that for the pin with 10% density; thus, the performance of the pin with 10% density was better. As shown in Fig. 7, at 47.8 rpm (0.14 m/s), the plot for the pin with 10% density intersects with those for the other pins. It indicates that the friction coefficient of the 10% pin has a greater tendency to decrease, especially at high velocities.

The minimum friction coefficient is generally seen in the sliding speed range 0.1-0.18 m/s (28.7-66.9 rpm), which corresponds to the mixed friction condition. Hydrodynamic or liquid friction is fully developed when the sliding speed is 0.22 m/s (86 rpm) or higher.

3-2. Scanning electron microscope image

Fig. 10 shows the scanning electron microscope (SEM) images of the dimpled pin after the test, under 23*x* and 800*x* magnification. Fig. 10 shows the image of the dimples. The pin surface is covered by dimples appearing as dots.

Under solid friction conditions, the dimples are in contact with the disk surface. The free area among the dimples acts as a reservoir. Paraffin oil, the lubricant is

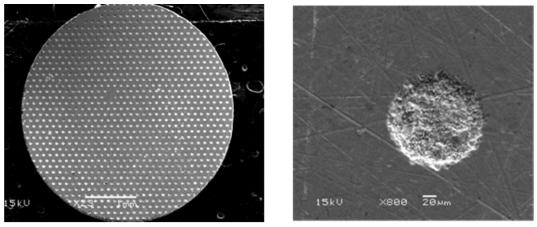

23 x 800x

Fig. 10. SEM image of dimpled pin (after test).

trapped in this area, resulting in some advantages [2]. The pressure provided by load increment at lower speeds compresses the lubricant, thereby causing the formation of a thin film between the contact surfaces.

The area that is not covered by dimples may act as a trap for worn fragments, so that these worn fragments are not welded into the contact surface. Small fragments are disadvantageous, potentially allowing for third-body contact.

4. Conclusion

In this study, we obtained the following results by performing frictional tests on a hexagonal array of 200 μm dimples:

1. The friction coefficient decreases with an increase in the sliding speed and load

2. The minimum friction coefficient is generally observed when the sliding speed ranges from 0.1 m/s to 0.18 m/s (28.7-66.9 rpm).

3. The pin with 15% dimple density shoes three friction regimes: solid, mixed, and fluid friction.

4. The friction coefficient of the sample with 10% dimple density is the most effective to reduce the friction for the velocity and load condition studied.

5. Hydrodynamic or liquid friction is fully developed when the sliding speed is 0.22 m/s (86 rpm) and higher.

References

[1] Nakada, M., "Trends in engine technology and tribology", *Tribology International*, Vol. 27, No. 1, pp. 3-8, 1994.

[2] Cho, M. H., Park, S., "Micro CNC surface texturing on Polyoxymethylene (POM) and its tribological performance in lubricated sliding", *Tribology International*, Vol. 44, pp. 859-867, 2011.

[3] Kato, A., Yasuda, Y., "An analysis of friction reduction techniques for the direct-acting valve train system of a new-generation lightweight 2-Liter V6 Nissan engine", *SAE Paper* No. 940992, 1994.

[4] Ronen, A., Etsion, I., Kligerman, Y., "Friction-reducing surface texturing in reciprocating automotive components", *Tribology Transaction*, Vol. 44, No. 3, pp. 359-366, 2001.

[5] Hamilton, D. B., Walowit, J. A., Allen, C. M., "A theory of lubrication by micro-irregularities", *J. of Basic Engineering*, March, pp. 177-185, 1966.

[6] Kim, D. H., Kim, J. K., Hwang, P., "Anisotropic tribological properties of the coating on a magnetic recording disk", *Thin Solid Films*, Vol. 360, pp. 187-194, 2000.

[7] Etsion, I., Kligerman, Y., Ghalperin, "Analytical and Experimental investigation of laser-textured mechanical seal faces", *Tribology Transactions*, Vol. 42, No. 3, pp. 511-516, 1999.

[8] Wang, X., Kato, K., Adachi, K., "The lubrication effect of micro-pits on parallel sliding faces of SiC in water", *Lubrication Engineering*, Aug., pp. 27-34, 2002.

[9] W. S. Choi, C. S. Jang, Y. H. Chae, "Friction characteristics of hexagonal array micro scale dimple pattern by density", *J. Korean Soc. Tribol. Lubr. Eng.*, Vol. 21, No. 6, 2008.

[10] Scaraggi, M., Mezzapesa, F. P., Carbone, G., Ancona, A., Sorgente, D., Lugara, P. M., "Minimize Friction of Lubricated Laser-Microtextured-Surface by Tuning Microholes Depth", *Tribology International*, Vol. 75, pp. 123-127, 2014.

[11] Wakuda, M., Yamauchi, Y., Kanzaki, S., Yasuda, Y., "Effect of surface texturing on friction reduction between ceramic and steel materials under lubricated sliding contact", *Wear*, Vol. 254, pp. 356-363, 2003.

[12] Jacobson, B., "The stribeck memorial lecture", *Tribology International*, Vol. 36, pp. 781-789, 2003.

[13] Woydt, M., Wäsche, R., "The history of the Stribeck curve and ball bearing steels: The role of Adolf Martens",*Wear*, Vol. 268, pp. 1542-1546, 2010.

[14] Yuriko, K., Tahahiro, K., Shinya S, "Tribological Properties of Ionic Liquids", Ionic Liquids - New Aspects for the Future, Dr. Jun-ichi Kadokawa (Ed.), ISBN: 978-953-51-0937-2, InTech, DOI: 10.5772/52595, 2013.